Applied Catalysis B: Environmental 254 (2019) 237–245

Contents lists available at ScienceDirect

Applied Catalysis B: Environmental

journal homepage: www.elsevier.com/locate/apcatb

Application of solar photocatalytic ozonation in water treatment using supported TiO_2

Eva M. Rodríguez*, Ana Rey, Estefanía Mena, Fernando J. Beltrán

Departamento de Ingeniería Química y Química Física, Instituto Universitario de Investigación del Agua, Cambio Climático y Sostenibilidad (IACYS), Universidad de Extremadura, Avda. Elvas S/N, 06006, Badajoz, Spain

ARTICLE INFO

Keywords:
Supported TiO_2
AOPs
Photocatalytic ozonation
Solar radiation
DEET
MWWTP secondary effluent

ABSTRACT

TiO_2 P25 supported on mullite ceramic foams (CF) and glass raschig rings (GR), have been prepared by dip-coating with calcination at 500 °C. The (photo) catalytic activity of these materials in the degradation of N, *N*-diethyl-m-toluamide (DEET) by different AOPs, in ultrapure water or in a secondary effluent, has been tested. Under the conditions applied, for a given process, the performance of CF and GR supported catalysts was similar, and a slight improvement was observed only from 1 to 2 TiO_2 coatings, indicating that, regardless of the support, after the second coating the amount of TiO_2 (2.4 and 0.49 wt% for CF and GR, respectively), was in excess with respect to the solar UV photon flux and/or the ozone entering the reactor. Ozonation was the most effective process for DEET and A_{254nm} removal, whereas solar photocatalytic ozonation led to the highest carboxylates formation and mineralization rates. At pH < 8.5, the presence of 5 mg L^{-1} PO_4^{3-} or 20 mg L^{-1} IC as HCO_3^-/$CO_3^=$ had no effect on DOC removal by this system, but some HO· scavenging effect was noticed when 40 mg L^{-1} IC was present, more markedly at pH > 8.5. The impact of the water matrix (ultrapure water, DOC_0 15 mg L^{-1}; or a secondary effluent, DOC_0 11 mg L^{-1} and IC_0 20 mg L^{-1}), on the effectiveness of photocatalytic oxidation was high, and low for photocatalytic ozonation (45–50% DOC removed from both matrices after 2 h). After several cycles of use, almost no loss of activity of the supported materials was observed. By comparing the characterization results of fresh/used materials their stability is deduced.

1. Introduction

Unit operations of wastewater treatment plants often do not eliminate organic micropollutants generated by human activities, mainly related to agriculture, health and personal care. Thus, compounds such as pharmaceuticals or pesticides, among others, are frequently found in municipal wastewater treatment plants (MWWTP) effluents, surface water and groundwater [1,2]. Since the late 1980's, combinations of ozone with different reagents (oxidants, catalysts, radiation) have been widely applied as advanced oxidation processes (AOPs) to remove organics from water [3,4]. These processes generate hydroxyl radicals ($HO^{\cdot}$), extremely short-lived oxidizing species that react non-selectively with the organics (and some inorganics) present in water. In addition, ozone reacts selectively, fast and directly with many organics compounds [4,5]. Thus, the interest of ozone processes in water treatment is based on these two routes to remove pollutants.

In AOPs, the concentration of hydroxyl radical generated is a key question, since the presence of many $HO^{\cdot}$ scavenging substances (e.g. carbonates) may render the process useless for contaminants removal. Hence, new combinations of ozone with other agents are being continuously investigated. Photocatalytic ozonation is one of these processes. It is based on the synergism between ozonation and photocatalytic oxidation (oxygen/radiation/catalyst), that may trigger different ways of $HO^{\cdot}$ formation [6–8]. More recently, one variation of this process is solar photocatalytic ozonation (SPO) that uses the solar light, natural or simulated, as UV source. Literature starts to publish works on this subject and some review has already appeared [9].

TiO_2 in suspension is probably the best option as photocatalyst, being the main drawback its separation from the solution at the end of the treatment. The use of supported TiO_2 would overcome this drawback, although an important decrease in photocatalytic activity is expected. Curiously, the first work published on the application of photocatalytic ozonation in water treatment deals with TiO_2 TP-2 (anatase) supported on glass tubes, using a low-pressure Hg lamp [10]. More recently, some authors have combined O_3/UV-A and supported materials to avoid the problem of catalyst-water separation [11–14]. Although UV-A radiation is part of that the Sun emits and reaches the Earth surface, just a few works have been published about SPO with

* Corresponding author.
E-mail address: evarguez@unex.es (E.M. Rodríguez).

https://doi.org/10.1016/j.apcatb.2019.04.095
Received 28 September 2018; Received in revised form 28 April 2019; Accepted 29 April 2019
Available online 30 April 2019

natural or simulated solar radiation. As far as we know, only Oyama et al. have investigated this system using TiO_2 P25, in suspension and immobilized on the inner surface of the glass tubes, for the removal of different organics in deionized water [15].

N,*N*-diethyl-m-toluamide (DEET), a key active ingredient in many insect repellent used mainly for direct application on the skin, is one of the most relevant compounds identified in EU MWWTP effluents, in terms of frequency of detection (100%), as well as maximum, average and median concentration levels (15.8 μg L^{-1}, 678 ng L^{-1} and 195.8 ng L^{-1}, respectively) [16]. Approximately 79% of DEET that enters the environment is associated to receiving waters directly from washing of skin and laundering of clothing, and indirectly via MWWTP discharges [17]. Due to its widespread use, DEET is commonly found in surface water and sediments at recreational bathing sites. Moreover, it was detected in 86% of drinking water catchment sites analyzed in Australia (maximum concentration 20 ng L^{-1}) [18].

Taking into account all the above, supported SPO is a very incipient AOP that deserves investigation, so the objectives of this work were: i) Preparation and characterization of TiO_2 P25 supported catalyst; ii) Determination of the efficiency of supported SPO on DEET degradation in ultrapure water, and comparison of results with the individual processes (ozonation, photocatalytic oxidation, ozone photolysis, etc.); and iii) Application of supported SPO in the treatment of a secondary effluent from a MWWTP.

2. Experimental section

2.1. Supported catalyst preparation

Two materials were used as support: glass raschig rings (GR) (6 × 6 mm) from Alamo (Spain), and ceramic foam filters (CF) VUKOPOR$^{(R)}$ made of mullite (Al_2O_3/SiO_2) from Lanik (Czech Republic). This latter material, with a cell density of 20 ppi (pores per inch), had a nominal size 50 × 50 × 22 mm. In this work, 30 mm diameter × 22 mm thick pieces were prepared from the commercial ones. Immobilization of TiO_2 onto GR or CF was carried out by the dip-coating procedure using a ND-DC dip-coater with 4 positions (Nadetech). Previously, CF pieces were washed several times with boiling ultrapure water and dried in a stove. Rugosity of GR pieces was increased washing with a 200 g L^{-1} potassium hydroxide ethanolic (KOH/EtOH) solution, then rinsing several times with ultrapure water and finally drying in a stove.

The coating suspension containing 150 g L^{-1} of TiO_2 P25 (Evonik) was prepared in ultrapure water at pH 1.5 (with HNO_3). The coating conditions were as follows: immersion/withdrawal at 0.65 mm s^{-1}, drying at 110 °C/24 h, and calcination at 500 °C/2 h (heating rate 5 °C min^{-1}). Consecutive cycles (1–3) of immersion/withdrawal + drying + calcination were applied when needed. After calcination, the support was rinsed several times with ultrapure water, dried in a stove and keep until use. Nomenclature used for the different prepared catalyst was CF (or GR)-TiO_2 (N), with N being the number of coatings.

2.2. Experimental set-up

The experimental set-up (see Fig. S1 in Supplementary information), consisted of an external agitated tank (V = 1.2 L) of borosilicate glass, with inlets and outlets for gases and sampling. The tank was filled with 1 L of water: 20 mg L^{-1} DEET in ultrapure water; or the secondary effluent from the MWWTP located in Badajoz (Spain) spiked with 1 mg L^{-1} of DEET. A peristaltic pump sent the water (10 L h^{-1}) from the external tank to the photoreactor in recirculation mode. The photoreactor was a borosilicate glass cylinder (3.5 cm i.d., 15.5 cm exposed length, total irradiated volume 0.17 L), packed with the catalyst (0.06 L GR + 0.11 L water; or 0.03 L CF + 0.14 L water), and placed inside the solar simulator (Suntest CPS, Atlas) provided with a 1500 W Xe lamp working at 550 W m^{-2}. All experiments were at room temperature. After 5 h, the increase of water temperature was lower than 5 °C.

Ozone was produced from pure oxygen (> 99.5%, Linde) by an Anseros Ozomat Com AD-02 generator. The O_2-O_3 mixture (flow rate 15 L h^{-1}; 15 mg L^{-1} O_3), was fed to the tank by means of a Teflon diffuser. The solution was first recirculated through the system in the dark for 15 min, to achieve adsorption equilibrium conditions. Then, O_2 or O_2-O_3 was fed and/or the Xe lamp turned on. From this moment, at different times, samples were taken from the tank and the photoreactor outlet. After purging dissolved ozone with air, the samples were filtered (0.2 μm PVDF Millipore) and analyzed. At the end of each experiment, the installation was emptied and thoroughly washed with ultrapure water.

2.3. Characterization of materials

Supports and supported catalysts were analyzed by different characterization techniques. Wavelength dispersive X-Ray fluorescence (WXRF) was used to determine the composition of the supports and the TiO_2 content in some materials. X-Ray diffraction of CF support was carried out in a Bruker D8 Advance XRD diffractometer. Surface areas were obtained from nitrogen adsorption-desorption isotherms at -196 °C acquired with an Autosorb iQ2-C (Quantachrome). Morphology and topography of supports and catalysts was characterized by scanning electron microscopy (SEM), using a Hitachi S-4800 (see more details in **Text T1,** SI).

2.4. Efficiency of oxidation treatment

DEET concentration was analyzed by HPLC-DAD (Hitachi, Elite LaChrom). Total dissolved organic carbon (DOC), and inorganic carbon (IC), were determined using a Shimadzu TOC-VSCH analyzer. Aqueous ozone concentration (in the tank and at the photoreactor outlet) was immediately measured by the indigo method [19,20]. Ozone in the gas phase was monitored by means of an Anseros Ozomat GM-6000 Pro analyzer. H_2O_2 concentration was determined by the cobalt/bicarbonate method [21]. Short-chain organic acids and inorganic anions were analyzed by Ion chromatography with chemical suppression (Metrohm 881 Compact Pro) and conductivity detection. For the characterization of the secondary effluent (SE) from the MWWTP, COD and N_{Total} were measured using Hach Lange test kits, N-NH_4^+ using a Spectroquant® test kit (Merck), and BOD_5 using an OxiTop® device [22] (see more details in **Text T1**).

3. Results and discussion

3.1. Characterization of materials

Elemental composition (wt%) of CF as oxides was: 68.6% Al_2O_3, 26.8% SiO_2 y 1.76% MgO. Other elements (Na_2O, K_2O, TiO_2 and Fe_2O_3 among others) also appeared but at percentages < 0.6%. The presence of mullite was confirmed from its structure determined with XRD. Corindon cristalline phase of Al_2O_3 was also observed (see XR diffractogram in Fig. S2).

Elemental composition of GR was: 68.5% SiO_2, 14.2% Na_2O, 5.42% CaO, 3.77% Al_2O_3, 3.22% K_2O, 2.47% MgO and 2.29% BaO. Other elements also appeared (Fe_2O_3, As_2O_3 and TiO_2) at percentages < 0.06%. Washing of GR with KOH/EtOH did not alter the composition of the material.

According to the specific surface area of the supports (Table 1), both resulted to be non-porous. S_{BET} of CF was 0.412 $m^2 g^{-1}$ with no variations after water washing. For GR S_{BET} was < 0.1 $m^2 g^{-1}$ and will practically correspond to the external surface area of the ring. No changes in S_{BET} were observed after washing with KOH/EtOH, although the development of a certain roughness was deduced from the analysis of SEM images (see in Fig. S3 two micrographs of GR before/after washing).

Table 1
S_{BET}, TiO_2 content (wt%) of supports and supported catalysts and size of TiO_2 layer.

Material	S_{BET} ($m^2\,g^{-1}$)	TiO_2 (%)[b]	Size of TiO_2 layer (μm)[c]
CF	0.412	n.m.[a] / 0.56	–
CF (washed)	0.460	n.m. / 0.58	–
CF-TiO_2(1)	n.m.	1.26 / n.m.	n.m.
CF-TiO_2(2)	n.m.	2.41 / n.m.	n.m.
CF-TiO_2(3)	1.925	3.08 / 6.10	3.3-20
CF-TiO_2(3) (used)	2.103	2.87 / 16.91	3.6-19.4
GR	< 0.1	n.m. / 0.01	–
GR (washed)	< 0.1	n.m. / < 0.005	–
GR-TiO_2(1)	n.m.	0.35 / n.m.	n.m.
GR-TiO_2(2)	n.m.	0.49 / n.m.	n.m.
GR-TiO_2(3)	0.123	0.52 / 0.43	5–23
GR-TiO_2(3) (used)	0.185	0.55 / 0.60	6.3–35.7

[a] n.m.: not measured.
[b] Gravimetric / WXRF results.
[c] Range of thickness observed by SEM.

Percentages of TiO_2 (wt%) on washed materials are also shown in Table 1. These values were obtained by gravimetric calculations (difference in weight before/after each coating), and for TiO_2(3) samples also with the use of WXRF. TiO_2 content in CF was: 1.26%, 2.41% and 3.08% for CF-TiO_2(1), CF-TiO_2(2) and CF-TiO_2(3). For CF-TiO_2(3), the great difference between gravimetric and WXRF values is likely due to the heterogeneous distribution of TiO_2 as confirmed by SEM analysis (see later). The slight increase in S_{BET} for CF-TiO_2(3) compared to bare CF would be related to the presence of around 3% of TiO_2-P25 (S_{BET} 50 $m^2\,g^{-1}$).

The amount of TiO_2 supported on GR was: 0.35%, 0.49% and 0.52% for GR-TiO_2(1), GR-TiO_2(2) and GR-TiO_2(3), respectively. Results obtained with WXRF for GR-TiO_2(3) are consistent with those from gravimetry, suggesting a more homogeneous distribution of TiO_2 on GR compared to CF. Addition of TiO_2 on GR also resulted in a slight increase of S_{BET}. The lower percentage of TiO_2 in GR compared to CF would be related to its lower S_{BET} and adherence in spite of the previous KOH/EtOH washing treatment.

TiO_2 distribution in both materials was analyzed by SEM (see Figs. S4-S6). In the case of CF, the surface of the raw material showed a homogeneous roughness (Fig. S4), and after TiO_2 incorporation a clear difference was seen respect to the support (Fig. S5), TiO_2 forming a smoother but fractured surface. From SEM images, TiO_2 layer thickness between 5–23 μm was observed. TiO_2 was deposited on GR surface forming a non-regular layer upon different ring zones (Fig. S6), thickness varying between 3.3–20 μm. The presence of fractures due to dryness and calcination was also observed. In summary, TiO_2 distribution was irregular for both materials.

3.2. Application of different AOPs in the elimination of DEET in ultrapure water

3.2.1. Solar photocatalytic oxidation

In an aerated solution and under radiation of appropriated wavelength, photoexcitation of TiO_2 leads to the appearance of different reactive oxygen species (ROS), through the simplified mechanism of reactions (1)–(6). In the case of TiO_2 P25, composed of anatase (bandgap 3.2 eV) and rutile (bandgap 3.0 eV) (anatase/rutile ratio of 5.3 ± 0.28), it is able to absorb radiation of wavelength up to approximately 400 nm [23].

$$TiO_2 \xrightarrow{h\nu} TiO_2 + h^+ + e^- \quad (1)$$

$$O_2 + e^- \xrightarrow{k=1.9x10^{10}\,M^{-1}s^{-1}} O_2^{\bullet -} \quad (2)$$

$$HO_2^{\bullet} \overset{pKa=4.8}{\rightleftarrows} O_2^{\bullet -} + H^+ \quad (3)$$

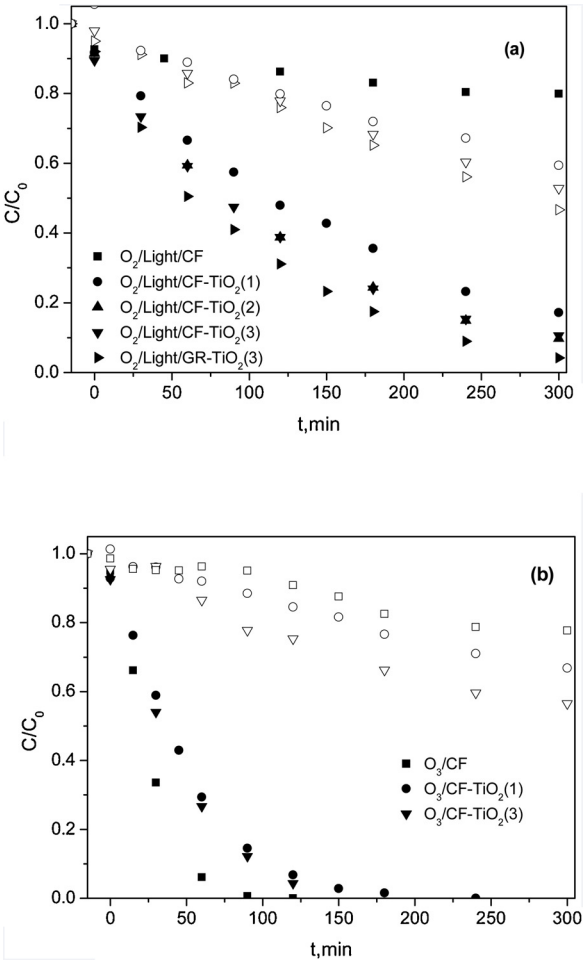

Fig. 1. Evolution of normalized concentration of DEET (solid) and DOC (open) with time during degradation of DEET by (a) photolytic and photocatalytic oxidation; (b) ozonation and catalytic ozonation. Experimental conditions: $C_{DEET,0}$ = 20 mg L^{-1}; $C_{DOC,0}$ = 15 mg L^{-1}; pH_0 ~ 6 (natural pH); Q_{O2} or Q_{O2-O3} = 15 L h^{-1}; $C_{O3g,0}$ = 15 mg L^{-1}; T = 20–25 °C; I_{solar} = 550 W m^{-2}.

$$2O_2^{\bullet -} + 2H^+ \rightarrow H_2O_2 \quad (4)$$

$$O_2^{\bullet -} + H_2O_2 \rightarrow HO^{\bullet} + OH^- + O_2 \quad (5)$$

$$H_2O_2 + e^- \xrightarrow{k=1.1x10^{10}\,M^{-1}s^{-1}} HO^{\bullet} + OH^- \quad (6)$$

Photocatalytic activity of the prepared materials was determined under simulated solar radiation, using DEET (20 mg L^{-1}) as probe compound at natural pH (pH_0~6). Fig. 1**(a)** shows changes with time of normalized DEET and DOC concentration in some experiments conducted with bare and TiO_2 coated materials. After 15 min of contact in the dark, DEET adsorption onto these materials was very low (~ 10%). The removal of DEET by O_2/Light/(CF or GR) was also low (~ 10% after 5 h), indicating that at the conditions tested TiO_2 present in raw CF (~ 0.56%, see Table 1) did not exert photocatalytic activity, and also, as expected, the absence of solar direct photolysis of DEET (see Fig. S7). DEET removal rate slightly increased from one to two TiO_2 coatings, with no further variations, and a similar behavior was observed in terms of DOC. For CF, the apparent pseudo-first order rate constant of DEET removal ($k_{Obs\text{-}DEET}$) was found to be 0.0055 min^{-1} and 0.0072 min^{-1} (R^2 > 0.99) for 1 and 2&3 TiO_2 coatings, respectively, and similar tendencies were found for GR (a slight increase in $k_{Obs\text{-}DEET}$ from 1 to 2 coatings and null effect of a third one). Therefore, under the experimental conditions applied, there was no correlation between TiO_2 content (Table 1) and the photocatalytic activity of the materials.

Comparing the different supports, DEET removal rate using TiO_2(3)

was slightly higher for GR ($k_{Obs\text{-}DEET}$ 0.0097 min^{-1}; $R^2 > 0.99$), whereas differences in mineralization rate were not significant, being DOC reductions after 5 h 47% and 53% for CF-TiO_2(3) and GR-TiO_2(3), respectively. Variation with time of carboxylates (acetate, formate, oxalate and pyruvate) was also very similar, their concentration being < 0.5 mg L^{-1} in all cases but acetate that reached up to 2 mg L^{-1}. From experiments performed by recirculating in the dark an aqueous mixture of carboxylates (5 mg L^{-1} each, pH 6; not shown), their adsorption onto the materials can be disregarded. The low specific surface area of the materials justifies these results (see Table 1). H_2O_2 concentration was also low (< 2×10^{-5} M), so that, at the conditions tested (oxygen-saturated solution) a significant contribution of reaction (6) is not expected.

Considering the mass of each supported catalyst inside the reactor, their TiO_2 content (%wt.) and the volumetric fraction of water, the amount of TiO_2 per volume of water in the photoreactor was ~ 5.7 g L^{-1} for CF-TiO_2(3) and ~ 6.4 g L^{-1} for GR-TiO_2(3), which could explain why GR-TiO_2(3) showed a slightly higher activity than CF-TiO_2(3). However, the fact that these differences were small, and taking into account the low influence of the number of coatings, the results suggest that, for both CF and GR, after the second coating the amount of TiO_2 exposed to light was in excess with respect to the solar UV photon flux reaching the system.

It must be highlighted that the experimental set-up is not optimized for its use in water treatment by supported photocatalytic oxidation. It is a simple and previous design that allows combining photocatalytic oxidation and ozonation to determine possible synergies between these systems. Thus, at a given moment, only 0.11 L or 0.14 L of solution (from a total volume of 1 L) is irradiated when using GR or CF materials, respectively. This means that, after 5 h treatment, the actual time one DEET molecule spent in the photoreactor was 33 min (GR) and 42 min (CF). With this in mind, the results in terms of DEET and DOC removal are comparable or even better than those obtained by Antonopoulou et al. [24], during the photocatalytic treatment of DEET (10 mg L^{-1}) using TiO_2 P25 in powder form (100 mg L^{-1}) and simulated solar light operating at 750 W m^{-2}.

3.2.2. Ozonation and catalytic ozonation

Due to its high oxidizing and disinfectant power, ozone is widely used in drinking water treatment and also as tertiary treatment method in wastewater depuration. Ozone acts in water in a double way: direct reaction with organic molecules and indirect reaction, where hydroxyl radicals, generated from its decomposition, are the oxidizing agents. Ozone decomposition can be promoted by different substances (oxidants, catalysts) and/or radiation [5], as it is the case of hydroxide anion (OH^-), which triggers the mechanism given by reactions (7)–(12) [25]. Similarly, different studies have shown the ability of TiO_2 (both in powder form or supported) to decompose ozone in water, in the dark, and promote the formation of ROS in some extent [11,26,27].

$$O^3 + OH^- \xrightarrow{k=70\,M^{-1}s^{-1}} HO_2^- + O^2 \quad (7)$$

$$O^3 + HO_2^- \xrightarrow{k=2.8x10^6\,M^{-1}s^{-1}} HO^\bullet + O_2^{\bullet -} + O^2 \quad (8)$$

$$HO_2^\bullet \overset{pKa=4.8}{\rightleftarrows} O_2^{\bullet -} + H^+ \quad (9)$$

$$O_3 + O_2^{\bullet -} \xrightarrow{k=1.6x10^9\,M^{-1}s^{-1}} O_3^{\bullet -} + O_2 \quad (10)$$

$$O_3^{\bullet -} + H^+ \xrightarrow{k=5.2x10^{10}\,M^{-1}s^{-1}} HO_3^\bullet \quad (11)$$

$$HO_3^\bullet \xrightarrow{k=1.1x10^5\,s^{-1}} HO^\bullet + O_2 \quad (12)$$

$$H_2O_2 \overset{pKa=11.6}{\rightleftarrows} HO_2^- + H^+ \quad (13)$$

Depending on whether the reactivity of ozone with the contaminants is low or high, the presence of promoters will have a beneficial or negative effect, respectively. DEET reactivity with ozone is low ($k_{O3\text{-}DEET}$ = 4.24 ± 0.17 $M^{-1}s^{-1}$ at 25 °C [28]), so that, *a priori,* decomposition of ozone into HO· is expected to have a positive effect on DEET removal ($k_{HO\text{-}DEET} = 4.95 \times 10^9$ $M^{-1}s^{-1}$ [29]). However, probably due to the presence of an amine group in DEET, this compound acts as a promoter of ozone decomposition [5,11], and at pH 6 both O_3 and HO· significantly contribute to DEET degradation [28]. Although H_2O_2 is formed from DEET-O_3 interaction (~ 1 mol of H_2O_2 per mol of DEET removed), and the ionic form of H_2O_2 (HO_2-, equilibrium (13)) can also promote ozone decomposition through (8), Mena et al. observed that, at pH 6, H_2O_2 accumulated in water and did not start to disappear until DEET was almost completely removed [28].

To determine if the prepared materials were active in terms of O_3 decomposition and generation of ROS, a new experimental series was carried out by combining ozone with the different catalysts. Previous assays indicated that bare CF or GR did not show catalytic activity, their presence only affecting the hydrodynamic of the system.

Fig. 1**(b)** shows changes with time of normalized concentration of DEET and DOC in some experiments using bare and TiO_2-coated CF. The evolution of H_2O_2 and dissolved ozone concentration is depicted in Fig. S8. Similar results were obtained for GR materials. Regardless of the number of coatings (1–3), TiO_2 had a negative effect on DEET removal rate and H_2O_2 formation, and positive on DOC elimination. Thus, $k_{Obs\text{-}DEET}$ was reduced by half in presence of TiO_2 (from 0.044 min^{-1} for O_3/CF to 0.024 min^{-1} for O_3/CF-TiO_2(1–3); $R^2 < 0.99$ in all cases), which implies that the efficiency of TiO_2-ozone interaction in terms of ROS generation is lower than that of DEET-O_3. Since the latter is the way H_2O_2 is formed [28], in presence of TiO_2 formation of H_2O_2 was also reduced (Fig. S8(a)). The lower concentration of dissolved ozone at the photoreactor outlet (Fig. S8(b)), confirms the ability of TiO_2 to decompose ozone in the dark [11,26,27].

With regard to mineralization, after 5 h DOC removal increased from 20% for O_3/CF system, to 30% and 40% when CF-TiO_2(1) and CF-TiO_2(2&3) were used. From Figs. 1(b) and S8(a), it is deduced that H_2O_2 does not play a relevant role in DOC mineralization. On the other hand, given the low reactivity of most carboxylates of low molecular weight towards ozone, HO· is the main species involved in their oxidation to CO_2 and H_2O, so in absence of HO· carboxylates tend to accumulate in water. The analysis of the evolution of carboxylates in these experiments indicates that, compared to single ozonation: 1) catalytic ozonation favored the removal of oxalate, which is related to the role of oxalate as promoter of ozone decomposition into HO· through the formation of the carboxyl radical $CO_2^{\bullet -}$ [30,31] (see Fig. S9); 2) for the rest of detected carboxylates the differences were not significant; and 3) acetate was the major carboxylate, regardless of the presence of TiO_2.

Although, contrary to photocatalytic oxidation, in catalytic ozonation all supported TiO_2 could participate in ozone decomposition, the experimental results indicate that TiO_2 was likely in excess after two coatings.

3.2.3. Solar photolytic and photocatalytic ozonation

The higher oxidizing capacity of ozone/solar radiation system compared to single ozonation is attributed to some overlapping between ozone light absorption spectrum and solar radiation reaching Earth's surface. Ozone absorbs radiation of λ < 325 nm and generates $O(^1D)$ through (14), the quantum yield ($\varphi_{O(1D)}$) decreasing from ~ 0.9 (λ < 305 nm) to 0.08 (λ = 325 nm). Atomic oxygen formed, $O(^1D)$, reacts with water and yields HO· through (15) [32,33].

$$O_3 \xrightarrow{h\nu} O_2 + O(^1D) \quad (14)$$

$$O(^1D) + H_2O \rightarrow 2HO^\bullet \quad (15)$$

Although reaction (14) can develop even under radiation of

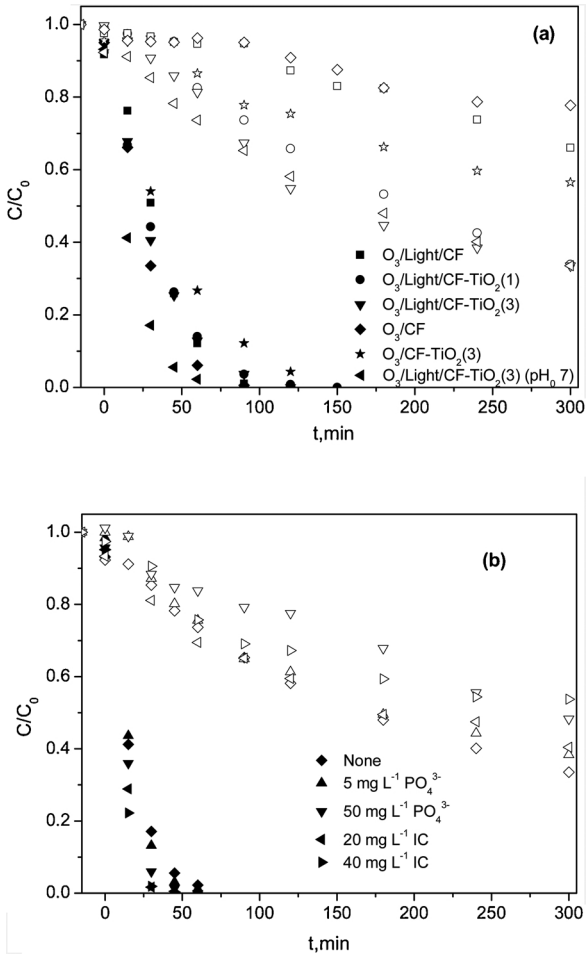

Fig. 2. Evolution with time of normalized concentration of DEET (solid) and DOC (open) during the application of (a) different O_3-based systems at pH_0 6 (except where indicated); (b) solar photocatalytic ozonation using CF-TiO_2(3), in absence/presence of different salts at pH_0 7. Experimental conditions: $C_{DEET,0}$ = 20 mg L^{-1}; $C_{DOC,0}$ = 15 mg L^{-1}; Q_{O2-O3} = 15 L h^{-1}; $C_{O3g,0}$ = 15 mg L^{-1}; T = 20–25 °C; I_{solar} = 550 W m^{-2}.

λ > 325 nm ($\varphi_{O(1D)}$ ~ 0.08 at 325–340 nm; $\varphi_{O(1D)}$ ~ 0.064 for 325–375 nm), molar absorptivity of ozone in these ranges is very low [33,34].

When ozone/solar radiation system is combined with TiO_2, (i.e., photocatalytic ozonation) formation of ROS can be incremented through two different mechanisms: 1) TiO_2 photoexcitation; and 2) interaction between TiO_2-O_3 in absence/presence of light. In the latter case, ozone can trap the photo-generated electrons giving rise to the ozonide ion radical ($O_3^{\cdot -}$) (reaction (16)) and, hence, to HO$^{\cdot}$ (reactions (11) and (12)) [10,35]:

$$e^- + O_3 \xrightarrow{k=6.3x10^{10} M^{-1}s^{-1}} O_3^{\cdot -} \quad (16)$$

If the concentration of ozone is very low compared to that of oxygen, reaction (16) could not compete with reaction (2), but ozone would still contribute to HO$^{\cdot}$ generation through (10)-(12) [36].

A new experimental series was carried out to check the efficiency of the ozone/light/supported catalyst systems. Fig. 2(a) shows, as an example, the changes with time of normalized concentration of DEET and DOC during some experiments with bare and coated CF. For comparative purposes, the results of O_3/CF and O_3/CF-TiO_2(3) systems are also included.

Ozonation (O_3/CF) and catalytic ozonation (O_3/CF-TiO_2) led to the highest and lowest $k_{Obs-DEET}$ (0.044 min^{-1} and 0.024 min^{-1}, respectively). For O_3/Light/CF, the initial degradation rate was lower than for O_3/CF, evidence of a certain decomposition of ozone. Nevertheless, DEET removal rate increased over time, and the time needed to achieve a 95% conversion was practically the same as for O_3/CF. For O_3/Light/CF-TiO_2, $k_{Obs-DEET}$ was about 0.035 min^{-1} regardless of the number of TiO_2 coatings, which indicates that the amount of ROS generated by photocatalytic ozonation is high enough to make up for the lower contribution of DEET-ozone interactions to DEET removal.

All systems resulted to be more effective than O_3/CF in terms of mineralization. After 5 h, DOC removed by O_3/CF was 20%, and increased to 30, 40 and 65% for O_3/Light/CF, O_3/CF-TiO_2(3) and O_3/Light/CF-TiO_2 systems, respectively. At that time, DOC removal was practically the same when using 1 or 3 coatings, although the contribution of carboxylates to residual DOC was slightly higher for TiO_2(3) (40% vs 30%), being acetate the major carboxylate (4 and 2 mg L^{-1} after 5 h, for 1 and 3 coatings, respectively), and remaining the concentration of the rest below 1 mg L^{-1}.

Since H_2O_2 is generated mainly from DEET-O_3 interaction, the higher the ozone decomposition the lower the H_2O_2 generated. Thus, during the first 100 min H_2O_2 formed by O_3/CF was slightly higher than for O_3/Light/CF, and much higher than for supported TiO_2 systems (see Fig. S10(a)). In any case, contribution of H_2O_2 to HO$^{\cdot}$ through reaction (6) would be very low compared to reactions (2) and (16). Generation of HO$^{\cdot}$ by H_2O_2 photolysis is not expected either due to its low molar absorptivity at λ > 310 nm (< 0.51 M^{-1} cm^{-1} [37]), its relatively low concentration (< 10^{-4} M), and the short period of UV exposure (33–42 min in total).

No doubt, ozone/light, with or without TiO_2, favors the decomposition of ozone and the formation, to a certain degree, of ROS. Thus, compared to O_3/CF, all combinations led to a decrease in dissolved ozone concentration at the photochemical reactor outlet (see Fig. S10(b)). For O_3/Light/CF-TiO_2 system, apart from O_3-light and O_3-TiO_2 interactions other ways of ROS generation are developed without ozone participation (i.e. semiconductor photoexcitation), which explains the higher mineralization achieved by this system despite the fact that concentration of ozone at the reactor outlet was similar to that of O_3/CF-TiO_2.

As in the case of photocatalytic oxidation (section 3.2.1) and catalytic ozonation (section 3.2.2), for photocatalytic ozonation the differences on the evolution of the different parameters analyzed using CF or GR supported catalysts were not significant (see Fig. S11).

The effect of pH on SPO was also tested using TiO_2(3). As an example, Fig. 2**(a)** includes the changes with time of DEET and DOC normalized concentration when CF-TiO_2(3) was used at pH_0 7 (not buffered). As observed, pH_0 had a clear positive effect on DEET removal rate, $k_{Obs-DEET}$ being 0.034 min^{-1} and 0.061 min^{-1} at pH_0 6 and pH 7, respectively. Since DEET is a neutral molecule, its reactivity towards ozone does not change with pH. The results indicate that an increase in pH favors the effective decomposition of ozone into HO$^{\cdot}$ through reactions (7)–(12). A higher pH_0 value also favored the oxidation of the first intermediates formed, as deduced if the formation rate of carboxylates of low molecular weight is compared, especially in the case of oxalate, although acetate continued to be the major one (see Fig. S12(a,b)). The influence of initial pH on mineralization was negligible, a logical result taking into account the evolution of pH with time (Fig. S12(c)). Since the medium was not buffered, the fast generation of carboxylic acids caused a pH drop to ~ 5.5 after 50 min of reaction in both cases, then increasing until reaching a value of ~ 6.5 after 5 h.

3.2.4. Influence of different anions on the efficiency of solar photocatalytic ozonation at pH 7

Although the presence of different ions in solution (carbonate, phosphate, chloride, etc.) may favor the aggregation or stabilization of catalyst particles, this effect is not relevant when working with supported catalysts [38–40]. However, these ions can alter the isoelectric point of the catalyst (IEP), diminish the photoproduction of positive holes and hydroxyl radicals by occupying active centers on the surface

of the catalyst, and compete with organic matter for the generated ROS [40,41].

To analyze the effect of different ions on the efficiency of solar photocatalytic ozonation, new experiments were carried out adding to the water: 1) the amount of phosphoric acid needed to obtain 5 or 50 mg L^{-1} of phosphate and, next, some drops of concentrated NaOH to reach pH 7; or 2) the amount of $NaHCO_3$ needed to obtain, after adjusting to pH 7 with some drops of concentrated HCl, a final concentration of inorganic carbon, IC, of about 20 or 40 mg L^{-1} (160 and 330 mg L^{-1} as $CaCO_3$ equivalents, respectively). According to equilibria (17) and (18), at pH 7 phosphate will be in the form of $H_2PO_4^-$ and $HPO_4^=$ at approximately equimolar concentrations, and the alkalinity mainly as bicarbonate, HCO_3^-.

$$H_3PO_4 \overset{pKa=2.1}{\rightleftarrows} H^+ + H_2PO_4^- \overset{pKa=7.2}{\rightleftarrows} 2H^+ + HPO_4^= \overset{pKa=12.4}{\rightleftarrows} 3H^+ + PO_4^{3-} \quad (17)$$

$$H_2CO_3 \overset{pKa=6.34}{\rightleftarrows} H^+ + HCO_3^- \overset{pKa=10.37}{\rightleftarrows} 2H^+ + CO_3^= \quad (18)$$

Fig. 2**(b)** shows, as an example, changes with time of normalized concentration of DEET and DOC during photocatalytic ozonation assays using CF-TiO_2(3). Evolution of pH, dissolved ozone concentration at the photoreactor inlet and outlet, and percentage of remaining DOC as carboxylates during these runs is shown in Fig. S13. In all cases H_2O_2 concentration was kept $< 2 \times 10^{-5}$ M. Similar results were obtained using GR-TiO_2(3).

According to Fig. 2(b), although after 60 min DEET was completely removed in all cases, $k_{Obs\text{-}DEET}$ increased in the presence of 50 mg L^{-1} of phosphate (˜ 0.09 min^{-1}; $R^2 < 0.99$), and when 20 or 40 mg L^{-1} IC was added (˜ 0.12 min^{-1}; $R^2 < 0.98$), being unaffected by the presence of 5 mg L^{-1} phosphate (˜ 0.06 min^{-1}; $R^2 < 0.99$). The influence of the different ions seems to be related to their effect on pH, as deduced from Fig. S13(a). Thus, the evolution of pH was similar when no salts or 5 mg L^{-1} phosphate was added, pH kept close to 7 in presence of 50 mg L^{-1} phosphate, and increased up to 8.3 and 8.7 within 60 min when 20 or 40 mg L^{-1} IC was present. The higher the pH, the greater the decomposition of ozone into HO· (see Fig. S13(b)), so differences in $k_{Obs\text{-}DEET}$ are mainly related to the effect of the salts on pH instead of their nature. Oxidation rate of the first reaction intermediates, in terms of DOC conversion into carboxylates, also increased with pH (Fig. S13(c)). An exception to the above was seen when 40 mg L^{-1} IC was added, with DOC conversion lower than for 20 mg L^{-1} IC, likely indicating some negative influence of alkalinity at these conditions. No direct relationship between pH and mineralization was observed, and after 5 h 60–65% DOC was removed in the absence of salts, with 5 mg L^{-1} phosphate or 20 mg L^{-1} IC. When 40 mg L^{-1} IC was added, after 60 min (once the pH reached 8.7), the mineralization rate slowed down, most probably due to the role of alkalinity as ROS scavenger, so after 5 h only 40% DOC was removed. If eq. (18) is considered, according to Fig. S13(a) alkalinity was mainly as HCO_3^-, with a certain amount of $CO_3^=$ that increased with pH. Both HCO_3^- and $CO_3^=$ can compete for HO˙ (reactions (19) and (20) [42]), with those compounds that exhibit low reactivity towards HO˙, or with high reactivity but at concentrations much lower than alkalinity. Hence, alkalinity/pH is an important aspect to consider in the treatment of MWWTP secondary effluents by any AOP.

$$HCO_3^- + HO^\bullet \xrightarrow{k=8.5x10^6 M^{-1}s^{-1}} CO_3^{\bullet -} + H_2O \quad (19)$$

$$CO_3^= + HO^\bullet \xrightarrow{k=4.2x10^8 M^{-1}s^{-1}} CO_3^{\bullet -} + OH^- \quad (20)$$

As a general rule, mineralization proceeds through the transformation of the organics into carboxylates of low molecular weight and their further oxidation. From the evolution of the different carboxylates (see Fig. 3), it is deduced that the increase in pH favors acetate and pyruvate removal, together with the accumulation of formate and oxalate, the latter becoming the major one at pH ≥ 8. Thus, for instance, in the experiment with 20 mg L^{-1} IC, where a higher pH did not improve mineralization (Fig. 2(b)), after 5 h formate and oxalate concentrations were 3.5 mg L^{-1} and 12 mg L^{-1}, respectively, and values lower than 1 mg L^{-1} were observed in absence of IC. If the rate constants of their reaction with HO˙ are considered ($k_{HO\text{-}oxalate}$ 7.7×10^6 M^{-1} s^{-1}; $k_{HO\text{-}formate}$ 3.2×10^9 M^{-1} s^{-1} [43]), together with those of reactions (19) and (20), oxalate accumulation could be related to the HO˙ scavenging effect of alkalinity, and even to a lower participation of holes in oxalate oxidation as a result of alkalinity-active centers interactions. In the case of formate (high $k_{HO\cdot}$ value), its accumulation would most probably be related to the lower contribution of O_3 direct reactions, since $k_{O3\text{-}formate}$ is several orders of magnitude higher than for the rest of detected carboxylates (100 M^{-1} s^{-1} [44]). To summarize, the beneficial effect of pH on HO˙ production and, therefore, in mineralization, can be reduced by alkalinity (on its role as HO˙ scavenger) and, in a lesser extent, by the lower contribution of ozone direct reactions.

Finally, in the experiment with 50 mg L^{-1} phosphate ($H_2PO_4^-$/$HPO_4^=$), where pH kept close to 7, a lower mineralization efficiency was observed from the beginning. Both H_2PO_4- and $HPO_4^=$ are refractory to ozone ($k_{O3} < 2x10^{-4}$ M^{-1} s^{-1} [45]), and their rate constants with HO˙ radicals are low ($2x10^4$ and 10^5 M^{-1} s^{-1}, respectively, [46]), so at the concentrations used in this work (< 0.5 mM) their role as HO˙ scavenger can be disregarded. The negative effect observed is likely related to their strong interaction with TiO_2 surface by occupying active centers [41,47]. In any case, according to our results and given the concentration of phosphate usually found in MWWTP secondary effluents, its presence is not expected to significantly affect the efficiency of SPO. Nonetheless, when used as buffer agent at high concentration, its possible effect on photocatalytic treatments should be considered [48].

To conclude this section, Fig. 4 shows, as a summary, $k_{Obs\text{-}DEET}$ values and percentages of mineralization reached at different reaction times for the most representative oxidation processes applied at pH_o 6 (Fig. 4**(a)**); and the effect of pH and presence of different anions on the efficiency of the combined O_3/Light/CF-TiO_2(3) system (Fig. 4**(b)**).

3.3. Application of different solar AOPs in the treatment of a secondary effluent from a MWWTP

In the last series of experiments, some of the studied processes were applied to treat the secondary effluent (SE) of the MWWTP of Badajoz (Spain), using CF-TiO_2(3) or GR-TiO_2(3) as catalysts. The effluent was previously filtered (Whatman Grade 1, 11 μm) and doped with 1 mg L^{-1} DEET. Main characteristics of SE were: pH 7.9; DOC 10 mg L^{-1}; IC 20 mg L^{-1}; A_{254} 0.19; N-total 8.5 mg L^{-1}; N-NO_3- 3.6 mg L^{-1}; DON 4.75 mg L^{-1} (see also Table T1 in SI).

As an example, Fig. 5 shows the evolution of different parameters during solar photolysis, photocatalytic oxidation, photolytic ozonation and photocatalytic ozonation of SE using CF-TiO_2 (3) as catalyst, working in the same conditions as in ultrapure water. The results obtained with GR-TiO_2(3) were practically coincident. Concentration of H_2O_2 kept $< 2 \times 10^{-5}$ M and pH remained in the range 8–8.4. For ozone-based systems, changes with time of $C_{O3,d}$ were similar, reaching after 90 min a stationary concentration of ˜ 2×10^{-5} M in the tank, and being $C_{O3,d} < 5 \times 10^{-6}$ M at the photoreactor outlet.

As observed in Fig. 5**(a)**, after 5 h, DEET removal due to direct/indirect photolysis was lower than 5%, so in case photosensitizing compounds are present in SE their effect on DEET removal was negligible. As expected, ozone systems (O_3/Light/CF y O_3/Light/CF-TiO_2(3)) led to a fast DEET removal (< 90% in less than 10 min) at similar rates ($k_{Obs\text{-}DEET}$ = 0.23 - 0.24 min^{-1}; $R^2 > 0.98$), much higher than O_2/Light/CF-TiO_2(3) ($k_{Obs\text{-}DEET}$ = 0.005 min^{-1}; $R^2 > 0.97$), for which, after 5 h (actual time 42 min), DEET concentration was reduced by 70%.

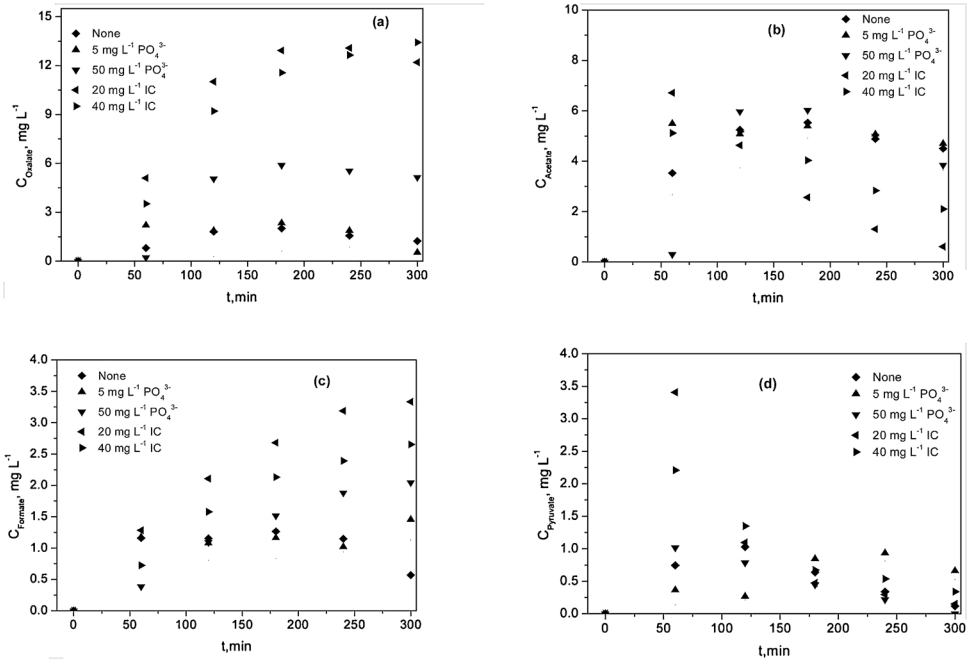

Fig. 3. Solar photocatalytic ozonation of DEET in ultrapure water using CF-TiO_2(3) at pH_0 7. Influence of the absence/presence of different anions on the evolution with time of (a) oxalate; (b) acetate; (c) formate ; (d) pyruvate. Same experimental conditions as in Fig. 2.

The role of ozone on aromaticity and unsaturated compound removal, measured as loss of absorbance at 254 nm (A_{254}), a proxy for aromaticity [4,49], is another point to highlight. As shown in Fig. 5**(b)**, regardless of the presence of catalyst, A_{254} decreased more than 90% after 100 min ($k_{Obs\text{-}A254}$ ˜ 0.033 min^{-1}; R^2 = 0.97), and was only reduced by half after 5 h of photocatalytic oxidation ($k_{Obs\text{-}A254}$ = 0.002 min^{-1}, R^2 > 0.99). Compounds with aromatic rings and unsaturated groups and hence high A_{254} values, have nucleophilic points in their structures where ozone, an electrophilic compound, reacts very fast through selective direct reactions [4,5]. Thus, it is not surprising the similar A_{254} profiles obtained in ozone processes since direct reactions are main responsible ways to remove these compounds. In the absence of ozone this way of reaction does not develop and A_{254} removal rate decreases significantly.

The main differences among ozone based processes was the evolution of the degree of oxidation of the intermediates (measured as DOC as carboxylates, %), and the mineralization (Fig. 5**(c)**). Thus, after 60 min (total DEET removal, A_{254} reduction > 80%, and no mineralization), DOC in solution as carboxylates was 23% and 30% for O_3/Light/CF y O_3/Light/CF-TiO_2(3) systems, respectively, and negligible for O_2/Light/CF-TiO_2(3). From 0 to 60 min, an initial increase in DOC content was observed due to the dissolution of some suspended organic matter present in the SE. From 60 to 120 min, DOC removal was important being the O_3/Light/CF-TiO_2(3) system the most active, and after 120 min the mineralization slowed down. Thus, after 2 h, DOC reduction attained was ˜ 12, 32 and 44% for O_2/Light/CF-TiO_2(3), O_3/

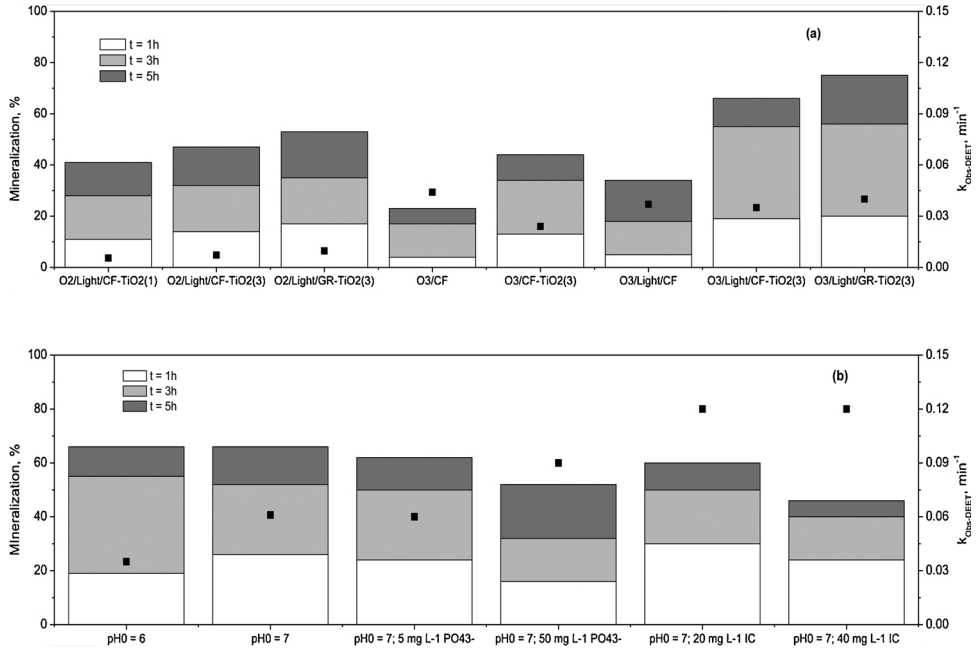

Fig. 4. Efficiency of DEET removal in ultrapure water as a function of $k_{Obs\text{-}DEET}$ (symbols) and % of DOC conversion at different times (bars). (a) Influence of the treatment applied at pH_0 6; (b) Influence of pH_0 and phosphate content and alkalinity on solar photocatalytic ozonation of DEET using CF-TiO_2(3) at pH_0 7. Experimental conditions: $C_{DEET,0}$ = 20 mg L^{-1}; $C_{DOC,0}$ = 15 mg L^{-1}; Q_{O2} or $Q_{O2\text{-}O3}$ = 15 L h^{-1}; $C_{O3g,0}$ = 15 mg L^{-1}; T = 20–25 °C; I_{solar} = 550 W m^{-2}.

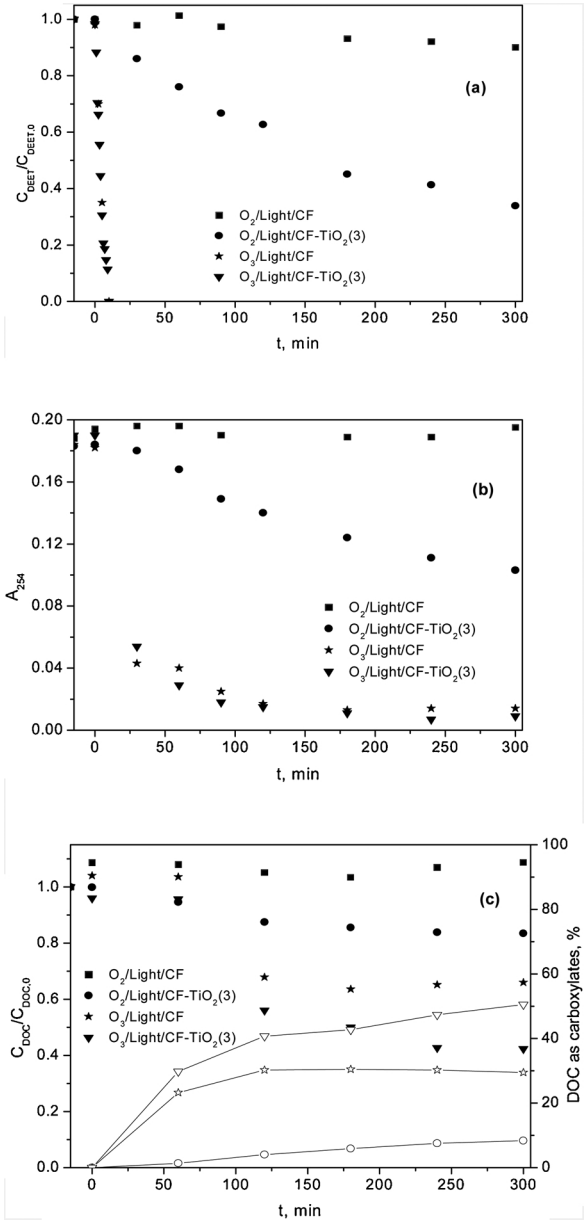

Fig. 5. Application of different processes on the treatment of the MWWTP secondary effluent spiked with 1 mg L^{-1} of DEET. Evolution with time of (a) normalized concentration of DEET; (b) A_{254}; (c) normalized concentration of DOC (solid) and % of DOC as carboxylates (open). Experimental conditions: $C_{DEET,0}$ = 1 mg L^{-1}; $C_{DOC,0}$ = 10.8 mg L^{-1}; pH_0 ~ 8; $A_{254,0}$ ~ 0.19; IC = 20 mg L^{-1}; $Q_{O2\text{-}O3}$ = 15 L h^{-1}; $C_{O3g,0}$ = 15 mg L^{-1}; T = 20–25 °C; I_{solar} = 550 W m^{-2} (see also Table T1 in SI).

Light/CF and O_3/Light/CF-TiO_2(3) systems, respectively; and ~ 17, 34 and 58% after 5 h, being DOC as carboxylates 10, 30 and 50%, respectively. As expected, given the pH of water (pH > 8), oxalate was the major one followed by formate, whereas the concentration of the rest remained below 1 mg L^{-1}.

The ability of these systems to reduce the dissolved organic nitrogen content (DON) was lower than for DOC. Thus, after 5 h, N-NO_3^- concentration remained the same during photocatalytic oxidation (~ 3.6 mg L^{-1}), and increased to 4.4 mg L^{-1} and 4.2 mg L^{-1} for photolytic ozonation and photocatalytic ozonation (Fig. S14). In all cases, NO_2^- kept under the LOD (0.2 mg L^{-1}), and N-NH_4^+ was < 0.3 mg L^{-1}. Taking into account the amount of DON in the SE (~ 4.7 mg L^{-1}), this means that, at the conditions applied and regardless of the presence of catalyst, ozone-based processes allowed to transform ~ 15% DON into NO_3^-, in agreement with the findings of Randtke et al., who determined that ozonation of SE leads to DON reductions of 14 ± 7% [50].

3.4. Reuse of materials and characterization

After having used CF-TiO_2(3) and GR-TiO_2(3) materials in the experimental series described in the previous sections, each material was used again in four consecutive replicas of SE photocatalytic ozonation, measuring the initial and final DOC values and determining the amount of DOC removed after 5 h. Differences found were lower than 15% in both cases. At a first sight, this could indicate that the materials were stable, with a low level of deactivation. However, since TiO_2 inside the photoreactor was probably in excess, the used materials were characterized and compared to the fresh ones. The results obtained are shown in Table 1. As observed, the amount of TiO_2 in used CF-TiO_2(3) was ~ 7% lower than in the fresh material (gravimetric results), which suggests that some TiO_2 was not strongly linked after calcinations and could have been detached out. In the case of GR-TiO_2(3), % of TiO_2 was practically the same before and after its use. Variations of BET specific surface of the materials after their use were not significant, and both morphology and topography of TiO_2 layers observed by SEM were similar (Figs. S15 and S16). Therefore, although the dip-coating procedure led to catalytic materials with an irregular distribution of TiO_2, both were stable and active. In our opinion, it is reasonable to think the results of this work are a good starting point for the use of these types of materials in the treatment of wastewater in continuous mode and on a larger scale.

4. Conclusions

TiO_2 supported on CF and GR materials have been prepared by dip-coating. The materials resulted to be efficient in the elimination of DEET from water and wastewater by different AOPs, some of them using solar light as UV source. At the conditions tested and regardless of the process applied, for each support no differences on the activity were observed when more than two TiO_2 coatings were applied. If CF and GR supported materials are compared, TiO_2 coated GR showed a slightly better performance. Combination of ozone with catalyst and/or solar radiation had a negative impact on DEET degradation rate, but positive on DOC transformation into carboxylates and their subsequent mineralization. In terms of mineralization, photocatalytic ozonation resulted to be the most effective process regardless of the water matrix. While an increase in pH accelerated DEET degradation by photocatalytic ozonation, its impact on DOC removal was low, acetate resulting to be the major carboxylate at pH ≤ 7 and oxalate at higher pH. The higher the pH, the lower the synergy between the systems was, due to the decomposition of ozone in water. At the concentrations commonly found in secondary effluents, phosphate is not expected to exert any influence on the effectiveness of the photocatalytic ozonation process, whereas bicarbonate/carbonate ions can act as HO· scavenger depending on the pH of the water and the alkalinity content. From the results obtained after several cycles of reuse, together with the characterization of the reused materials, the stability of the supported catalysts is deduced. The application of these systems as a tertiary treatment of secondary effluents from MWWTP in continuous mode and on a larger scale will be the subject of a future work.

Acknowledgements

This Special Issue is dedicated to honor the retirement of Prof. César Pulgarin at the Swiss Federal Institute of Technology (EPFL, Switzerland), a key figure in the area of Catalytic Advanced Oxidation Processes. Passionate about life and work and a great conversationalist, always ready for a fruitful discussion. The authors also thank the Spanish Ministry of Economy and Competitiveness, and the European Funds for Development (project CTQ2015/64944-R), for the economic

support.

Appendix A. Supplementary data

Supplementary material related to this article can be found, in the online version, at doi:https://doi.org/10.1016/j.apcatb.2019.04.095.

References

[1] S. Navarro, N. Vela, M.J. Gimenez, G. Navarro, Sci. Total Environ. 329 (2004) 87–97.
[2] M. Stuart, D. Lapworth, E. Crane, H. Hart, Sci. Total Environ. 416 (2011) 1–21.
[3] W.H. Glaze, J.W. Kang, D.H. Chapin, Ozone Sci. Eng. 9 (1987) 335–342.
[4] F.J. Beltrán, Ozone Reaction Kinetics for Water and Wastewater Systems, BocaRaton, CRC Press, Florida, USA, 2004.
[5] C. von Sonntag, U. von Gunten, Chemistry of Ozone in Water and Wastewater Treatment: From Basic Principles to Applications, IWA Publishing, London, UK, 2012.
[6] T.E. Agustina, H.M. Ang, V.K. Vareek, J. Photochem. Photobiol. C Photochem. Rev. 6 (2005) 264–273.
[7] M. Mehrjouei, S. Müller, D. Möller, Chem. Eng. J. 263 (2015) 209–219.
[8] J. Xiao, Y. Xie, H. Cao, Chemosphere 121 (2015) 1–17.
[9] F.J. Beltrán, A. Rey, Molecules 22 (2017) 1177.
[10] K. Tanaka, K. Abe, T. Hisanaga, J. Photochem. Photobiol. A Chem. 101 (1996) 85–87.
[11] M. Fathinia, A. Khataee, Appl. Catal. A Gen. 491 (2015) 136–154.
[12] N.F.F. Moreira, J.M. Sousa, G. Macedo, A.R. Ribeiro, L. Barreiro, M. Pedrosa, J.L. Faria, M.F.R. Pereira, S. Castro-Silva, M.A. Segundo, C.M. Manaia, O.C. Nunes, A.M.T. Silva, Water Res. 94 (2016) 10–22.
[13] G. Simon, T. Gyualavári, K. Hernadi, M. Molnár, Z. Pap, G. Veréb, K. Schrantz, M. Náfrádi, T. Alapi, J. Photochem. Photobiol. A Chem. 356 (2018) 512–520.
[14] R. Oblak, M. Kete, U. Lavrencic Stangar, M. Tasbihi, J. Water Proc. Eng. 23 (2018) 142–150.
[15] T. Oyama, T. Otsu, Y. Hidano, T. Koike, N. Serpone, H. Hidaka, Sol. Energy 85 (2011) 938–944.
[16] EU Report, (2012) http://publications.jrc.ec.europa.eu/repository/bitstream/JRC76400/lb-na-25563-en.pdf.pdf.
[17] J.A. Weeks, P.D. Guiney, A.I. Nikiforov, Integr. Environ. Assess. Manag. 8 (2012) 120–134.
[18] National Research Centre for Environmental Toxicology, The University of Queensland, Australia, 2016https://www.seqwater.com.au/sites/default/files/PDF%20Documents/Publications/Enclosure%202b%20-%202016%20Summer%20Catchment%20and%20Drinking%20Water%20Quality%20Micro%20Pollutant%20-%20Monitoring%20Program%20%E2%80%93%20Passive%20Sampling.pdf.
[19] H. Bader, J. Hoigné, Water Res. 15 (1981) 449–456.
[20] I. Ilisz, A. Bokros, A. Dombi, Ozone Sci. Eng. 26 (2004) 585–594.
[21] W. Masschelein, M. Denis, R. Ledent, Water Sewage Works (August) (1977) 69–72.
[22] OECD, Ready Biodegradability. Test Guideline 301, (1992).
[23] B. Ohtani, O.O. Prieto-Mahaney, D. Li, R. Abe, J. Photochem. Photobiol. A Chem. 216 (2010) 179–182.
[24] M. Antonopoulou, A. Giannakas, Y. Deligiannakis, I. Konstantinou, Chem. Eng. J. 231 (2013) 314–325.
[25] M.D. Gurol, P.C. Singer, Environ. Sci. Technol. 16 (1982) 377–383.
[26] R. Gracia, S. Cortés, J. Sarasa, P. Ormad, J.L. Ovelleiro, Ozone. Sci. Eng. 22 (2000) 185–193.
[27] J. Nawrocki, B. Kasprzyk-Hordern, Appl. Catal. B Environ. 99 (2010) 27–42.
[28] E. Mena, A. Rey, E.M. Rodríguez, F.J. Beltrán, Appl. Catal. B Environ. 202 (2017) 460–472.
[29] W. Song, W.J. Cooper, B.M. Peake, S.P. Mezyk, M.G. Nickelsen, K.E. O'Shea, Water Res. 43 (2009) 632–642.
[30] R. Andreozzi, A. Insola, V. Caprio, M. D'Amore, Water Res. 26 (1992) 917–921.
[31] C.D. Vecitis, T. Lesko, A.J. Colussi, M.R. Hoffmann, J. Phys. Chem. A 114 (2010) 4968–4980.
[32] D. Biedenkapp, L.G. Hartshorn, E. Bair, J. Chem. Phys. Lett. 5 (1970) 379–381.
[33] J.B. Burkholder, S.P. Sander, J. Abbatt, J.R. Barker, R.E. Huie, C.E. Kolb, M.J. Kurylo, V.L. Orkin, D.M. Wilmouth, P.H. Wine, Chemical Kinetics and Photochemical Data for Use in Atmospheric Studies, Evaluation No. 18, JPL Publication 15-10, Jet Propulsion Laboratory, Pasadena, 2015http://jpldataeval.jpl.nasa.gov.
[34] Y. Matsumi, F.J. Comes, G. Hancock, A. Hofzumahaus, A.J. Hynes, M. Kawasaki, A.R. Ravishankara, J. Geophys. Res. 107 (2002) ACH 1-1–ACH 1-12.
[35] L. Sánchez, J. Peral, X. Doménech, Appl. Catal. B Environ. 19 (1998) 59–65.
[36] P. Kopf, E. Gilbert, S.H. Eberle, J. Photochem. Photobiol. A Chem. 136 (2000) 163–168.
[37] L. Chu, C. Anastasio, J. Phys. Chem. A 109 (2005) 6264–6271.
[38] O. Autin, J. Hart, P. Harvis, J. MacAdem, S.A. Parsons, B. Jefferson, Water Res. 47 (2013) 2041–2049.
[39] D. Avisar, I. Horovitz, L. Lozzi, F. Ruffieri, M. Baker, M.L. Abel, H. Mamane, J. Hazard. Mater. 244–245 (2013) 463–471.
[40] J.F. Budarz, A. Turolla, A.F. Piasecki, J.Y. Bottero, M. Antonelli, M.R. Wiesner, Langmuir 33 (2017) 2270–2279.
[41] M. Abdullah, G.K.C. Low, R.W. Matthews, J. Phys. Chem. 94 (1990) 6820–6825.
[42] G.V. Buxton, A.J. Elliot, Radiat. Phys. Chem. 27 (1986) 241–243.
[43] G.V. Buxton, C.L. Greenstock, W.P. Helman, A.B. Ross, J. Phys. Chem. Ref. Data 17 (1988) 513–886.
[44] J. Hoigné, H. Bader, Water Res. 17 (1983) 185–194.
[45] J. Hoigné, H. Bader, W.R. Haag, J. Staehelin, Water Res. 19 (1985) 993–1004.
[46] P. Maruthamuthu, P. Neta, J. Phys. Chem. 82 (1978) 710–713.
[47] P.A. Connor, A.J. McQuillan, Langmuir 15 (1999) 2916–2921.
[48] P.A. Morozov, B.G. Ershov, Russ. J. Phys. Ch. A 54 (2010) 1136–1140.
[49] J. Wenk, M. Aeschbacher, E. Salhi, S. Canonica, U. von Gunten, M. Sander, Environ. Sci. Technol. 47 (2013) 11147–11156.
[50] S.J. Randtke, G.F. Parkin, J.V. Keller, J.O. Lechie, P.L. McCarty, EPA-600/2-78-030, (1978) https://nepis.epa.gov/Exe/ZyPDF.cgi/91017WQQ.PDF?Dockey=91017WQQ.PDF.